

Modified effective medium model for gas hydrate bearing, clay-dominated sediments in the Krishna-Godavari Basin

Sriram, G.^{1,2}, Dewangan, P.^{1*}, Ramprasad, T.¹

¹ CSIR-National Institute of Oceanography, Dona Paula, Goa, 403004, India

² Presently at National Centre for Antarctic and Ocean Research, Vasco-da-Gama, Goa, 403804, India

*Corresponding author email: pdewangan@nio.org

Abstract

During NGHP-Expedition-01, well logs were obtained for gas hydrate exploration in Krishna-Godavari (KG) offshore basin. These logs coupled with a suitable rock physics model can be used to understand the interaction between the sediment grains of unconsolidated marine sediments as well as with hydrate. In this paper, we study the friction-dependent effective medium model (EMM) to understand these grain interactions. The compressional (P) and shear (S) wave velocities of fluid saturated sediments are estimated using different friction parameters at Site NGHP-01-03, which represent the background fluid-saturated marine sediment, and are compared with the observed velocities derived from sonic logs. Our analysis shows that the shear velocity is over estimated for the Hertz-Mindlin contact theory [no-slip across the grain contact], but can be accurately estimated for the Walton's smooth contact model [zero friction across the grain contact]. It suggests that the background shear wave velocity need to be modeled without friction at the grain contact for unconsolidated marine sediments. Further, the friction-dependent EMM theory is tested at Site NGHP-01-07 which represents the load-bearing gas hydrate deposits in KG basin. The comparison between the gas hydrate saturations estimated from sonic and resistivity logs shows that saturations estimated from P-wave velocity match well with those estimated from resistivity and chloride anomaly and is largely independent of the frictional parameter. However, gas hydrate saturations estimated from shear wave velocity is overestimated in the absence of friction but agrees with the other estimates if an arbitrary small friction is included in the EMM. We further extended the friction-dependent EMM for multi-grain contact (clay + quartz + hydrate) in which the effective modulus of sediment matrix is estimated by accounting for all possible contact combinations among the grains like quartz-quartz (QQ), clay-clay (CC), clay-quartz (QC), quartz-hydrate (QH), clay-hydrate (CH), and hydrate-hydrate (HH). The gas hydrate saturations estimated from shear velocity assuming the same non-zero friction term are underestimated as compared to those estimated from P-wave velocity. Interestingly, the saturations estimated assuming zero-friction from both P- and S-wave velocities are comparable to each other and shows a good match with those estimated from resistivity logs and chloride anomalies. The proposed EMM with zero friction and mixed grain contact is able to predict the velocities of fluid-saturated sediments as well as gas hydrate bearing sediments in KG offshore basin.

Keywords: gas hydrate, rock physics, effective medium model, grain contact theory, NGHP Expedition-01

1. Introduction

Gas hydrate is a naturally occurring, crystallized solid composed of water and hydrocarbon gas (mainly methane) molecules and is stable within a zone of high pressure and low temperature in marine sediments known as the gas hydrate stability zone (GHSZ) (Sloan, 1998). The presence of gas hydrate is inferred from the analysis of seismic and logging data. In the seismic data, the presence of gas hydrate is manifested in the form of anomalous reflector known as bottom simulating reflector (BSR) which represents the interface between the overlying gas hydrate bearing sediments and underlying free gas bearing sediments (Hyndman and Spence, 1992; Singh et al., 1993). In well-log data, its presence is inferred from the increase in electrical resistivity and elastic velocities as compared to that of fluid saturated sediments.

In situ gas hydrate saturations can be estimated from the analysis of logging while drilling (LWD), wireline logs and pressure cores. In order to quantify gas hydrate, a relationship between the physical property and gas hydrate/free gas saturation is required. For example, Gas hydrate saturation can be estimated from resistivity data using Archie's equation (Archie, 1942). Likewise, various velocity models based on either empirical relationships or first principles are required for estimating saturations from sonic logs. Depending on the distribution of gas hydrate within the sediments, several rock physics models like the cementation theory (Ecker et al., 1998), effective medium model (EMM; Helgerud et al., 1999), effective medium theory using self-consistent approximation (SCA) and differential effective medium (DEM) (Jakobsen et al., 2000), modified Biot-Gassmann theory (Lee, 2002), three-phase Biot type equation (TPBE; Carcione and Tinivella, 2000; Guerin and Goldberg, 2005; Lee and Waite, 2008) are proposed. A general comparison among these models (Chand et al., 2004) suggests that different rock physics models exhibit similar P- and S-wave velocities for hydrate free sediments, but show marked difference in the velocities of gas hydrate bearing sediments.

Drilling/coring activities during National Gas Hydrate Program Expedition-01 (NGHP-01) has established the presence of gas hydrate in Krishna-Godavari (KG), Mahanadi and the Andaman basins (Collett et al., 2008; Collett et al., this volume; Kumar et al., this volume). In some cases, massive hydrate is visually observed in the sediment cores from KG basin. In most cases, pressure cores were deployed to confirm the presence of gas hydrate. Sedimentological data reveals that sediments in KG and Mahanadi basins are clay dominated with 85-95 % clay and 5-15 % silt (Collett et al., 2008).

Several rock physics theories have been formulated for gas hydrate bearing sediments in KG offshore basin. The pressure core X-ray images and resistivity at bit (RAB) images from Site NGHP-01-10, KG basin, show fracture-filled gas hydrate in clay dominated sediments (Collett et al., 2008). Based on this observation, Lee and Collett (2009) proposed an anisotropic rock physics model in which the effective properties of the medium are obtained using Backus average theory (Backus, 1962) for different gas hydrate saturations. The study of amplitude variation of BSR with incidence angle in the vicinity of site NGHP-01-10 also suggests that the medium is anisotropic and realistic gas hydrate saturation as well as fracture azimuth can be estimated assuming the anisotropic rock physics model (Sriram et al., 2013). In both of these studies, the TPBE (Lee and Waite, 2008) has been used to model the P- and S-wave velocities of the background clay dominated sediments. The TPBE model depends on a consolidation parameter (Pride et al., 2004) which is a function of pressure/depth and is obtained empirically so that the estimated background P-wave velocity is close to the observed velocity. Such empirical relationship is good for modeling velocities, but it does not give any insight into the physical interaction between the sediments and the gas hydrate. Therefore, we attempt to model the P- and S-wave velocities of clay dominated hydrate bearing sediments using the first principle based effective medium model (EMM) (Dvorkin et al., 1999; Helgerud et al., 1999). We first model the velocities from Site NGHP-01-03 which represents the baseline clay dominated sediment in KG offshore basin, and later model the velocities from Site NGHP-01-07 which represents gas hydrate bearing sediments. We deliberately choose Site NGHP-01-07 as it shows low fracture density and the gas hydrate may be represented by either pore-filling or load-bearing form of gas hydrate and not fracture-filled gas hydrate. The EMM is modified by incorporating inter-particle contact friction parameters (Duffaut et al., 2010; Bachrach and Avseth, 2008) and grain contact model (Hossain et al., 2011) so that the background velocities can be accurately estimated, and the gas hydrate saturations estimated from the sonic log are similar to those estimated from the resistivity log and core derived chloride profile.

2. Development in effective medium model (EMM) technique

The effective medium model (EMM) is based on the first principle physics (Dvorkin et al., 1999) where the effective elastic properties of the identical sphere packs are estimated using the Hertz-Mindlin contact theory (Mindlin, 1949). EMM is used to approximate the behavior of the granular media with many contacts using the average of two-grain contacts. Such contact theory accurately approximates the bulk modulus of sediment matrix, but fails to model the shear modulus (Bachrach and Avseth, 2008;

Duffaut et al., 2010). Several experimental studies have reported significant difference between the shear modulus estimated from Hertz–Mindlin contact theory and the laboratory measured shear modulus (Winkler, 1983; Goddard, 1990; Zimmer et al., 2007). The numerical granular dynamics model (Makse et al., 1999) suggests that the Hertz–Mindlin contact theory fails to predict the shear modulus because the grains tend to relax from the macroscopic deformation or rotate leading to the breakdown of uniform strain assumption. Accurate shear wave estimation is important for several geophysical studies such as reservoir modeling using amplitude variation with offset, vertical seismic profiling (VSP), and identification of the fluid type, lithology and other mechanical properties. Error in estimation of the S–wave velocity may lead to an error in Poisson’s ratio, impedance, V_p/V_s ratio and fluid factor.

The problem of incorrect S–wave velocity was addressed initially by Bachrach and Avseth (2008) by considering non–uniform contact and heterogeneous stress fields in effective medium. A binary scheme was introduced where the grain contact can be either smooth with zero tangential stiffness or no–slip with tangential stiffness estimated from Hertz–Mindlin contact theory. The effective elastic modulus is then estimated from the combination of smooth and no–slip contacts using a parameter f_t which represents the fraction of no–slip contact. Such binary model for grain contact gives more reliable estimate of shear modulus (Bachrach and Avseth, 2008). Duffaut et al. (2010) extended the EMM by introducing partial slip with nonzero contact friction and a free parameter, Mindlin friction term $f(\mu)$, which represents the ratio between the radii of the no–slip contact area and of the full contact area. In this frictional dependent model, the effective shear modulus of the identical sphere pack is derived by combining the tangential contact stiffness estimated from Mindlin’s theory (Mindlin, 1949) with the effective modulus expression derived by Digby (1981). The free parameters, Mindlin’s friction term (Duffaut et al., 2010) and the fraction of no–slip contact (Bachrach and Avseth, 2008), of the modified effective medium theories are estimated from the laboratory studies of dry bulk and shear moduli of core samples. The friction parameter $f(\mu)$ can also be estimated from the dry bulk and shear moduli (Duffaut et al., 2010; equation B1) calculated from sonic log using Gassmann’s equation (Gassmann, 1951). These models show similar estimates of bulk and shear moduli and match well with the stress–velocity data of glass beds and loose sand (Zimmer, 2003; Zimmer et al., 2007).

3. Log Data and Methodology

Several well logs were acquired in the clay dominated marine sediments in Krishna–Godavari basin for gas hydrate exploration (Collett et al., 2008). In this study, we have considered the Site NGHP–01–03 located in KG Basin (15°53.891' N, 81° 53.9678' E) at water depth of ~1076 m (Fig.1). At this site, negligible gas hydrate saturation has been reported from the analysis of resistivity logs as well as from the pressure core data (Collett et al., 2008); therefore, the site represents the properties of fluid–saturated marine sediments in KG offshore basin. The logging while drilling (LWD) data was recorded to a depth of 300 mbsf (meters below seafloor) and the BSR depth is at 209 mbsf. The quality of log data was evaluated from the caliper logs, and the zones of washouts are excluded from the data. The caliper data at site NGHP–01–03 shows occasional washouts, and overall the data quality is good. The porosity is derived from density log data measured with EcoScope tool and is in good agreement with the porosities estimated from core using moisture and density (MAD) analysis. We applied various modifications of EMM theory for estimating the P– and S–wave velocities at Site NGHP–01–03 and compared it with the observed velocities. Such comparisons help in understanding the grain–fluid interactions particularly in clay dominated environment. We also considered Site NGHP–01–07 (Fig. 1), which represents the pore–filling/load–bearing hydrate deposits in KG offshore basin, for studying the modified EMM theories for gas hydrate bearing sediment. Site NGHP–01–07 is located in northern part of the KG Basin (16° 31.2785' N, 82° 40.8572' E) at a water depth of 1285 m and the BSR depth is about 188 mbsf. The LWD data is recorded up to a target depth of 260 mbsf and some pressure cores were obtained for direct quantification of gas hydrate (Collett et al., 2008). The quality of P– and S–wave velocities as well as the resistivity log data is evaluated based on the caliper log data and in general, the quality of the data is good for estimating the gas hydrate saturation. The hydrate saturations estimated from P– and S–wave data are compared with those estimated from resistivity log and residual chloride concentration.

The general methodology for estimating the elastic velocities from porosity using modified EMM (Appendix A; after Dvorkin et al., 1999) is as follows: the effective bulk (K) and shear (G) moduli of different mineral constituents are estimated using Hill's average equation (Hill, 1952), the critical porosity is obtained from the crossplot of porosity and velocity data (Dvorkin et al., 1999), the dry bulk (K_{HM}) and shear (G_{HM}) moduli at critical porosity are estimated using the Hertz–Mindlin

contact theory with varying Mindlin's friction parameter $f(\mu)$ as discussed by Duffaut et al (2010) [Appendix B]. The dry elastic moduli of the shallow marine sediment at porosity larger than critical porosity, K_{Dry} and G_{Dry} are estimated using upper Hashin–Shtrikman bounds (1963). Likewise, the moduli are estimated using lower Hashin–Shtrikman bounds for porosities smaller than the critical porosity. The fluid saturated bulk modulus (K_{Sat}) is estimated from Gassmann (1951) equations (A5). The P- and S-wave velocities are estimated using equation (A6).

In the present study, we also model the P- and S-wave velocities of gas hydrate bearing sediment assuming the load-bearing form of gas hydrate. We ignore the pore-filling form of gas hydrate as it affects only P-wave velocity and S-wave velocity is unchanged; however, at Site NGHP-01-07 both P- and S-wave velocities increase with hydrate saturation. We adopted the method of Helgerud et al. (1999) where gas hydrate is considered to be a part of sediment matrix and the effective bulk and shear moduli are estimated using Hill (1952) equation by replacing the volume fraction f_i with \bar{f}_i (equation A7) which represents the new volume fraction due to the presence of gas hydrate. This effective bulk and shear moduli of the sediment matrix are used for the calculation of dry bulk and shear moduli which in turn are used to estimate the fluid saturated moduli. The P- and S-wave velocities are calculated for varying gas hydrate concentration using equation (A6).

4. Results and Discussion

The bulk and shear moduli of fluid saturated, clay dominated, unconsolidated marine sediments are estimated assuming different friction parameters in the EMM, and are compared with the observed moduli at Site NGHP-01-03. The same method is also used to estimate the moduli of gas hydrate bearing sediments at site NGHP-01-07 by varying friction parameter and also accounting for multiple grain contacts in EMM (Hossain et al., 2011). The calibration process provides the crucial information about the interaction between the sediment grains with or without the presence of gas hydrate.

4.1 Modified EMM for fluid-saturated marine sediments at Site NGHP-01-03

The effective bulk and shear moduli of the solid frame are estimated using Hill's average assuming ~95% clay and ~5% quartz as reported from smear slide data (Collett et al., 2008), and the elastic properties of individual mineral constituents are shown in Table-1 (Helgerud et al., 1999). The sediment porosities (52 – 60 %) estimated from density log show good agreement with those estimated

from core samples. At site NGHP-01-03, the critical porosity estimated from velocity-porosity crossplot is ~55 %. The coordination number, defined as an average number of contacts between individual grains, is estimated to be 5 based on the range of porosities (equation A3). The dry bulk and shear moduli at critical porosity are estimated for Walton's smooth model [$f(\mu)=0$] and for Hertz-Mindlin's no-slip model [$f(\mu)=1$]. The effective dry bulk and shear moduli are estimated using Hashin-Shtrikman upper and lower bounds (1963) (equation A4). The effective bulk modulus of fluid is calculated using the equation of Batzle and Wang (1992) assuming a fluid density of 1.038 g/cm³, temperature is estimated from the measured geothermal gradient, pressure is assumed to be hydrostatic pressure, and the salinity is assumed to be 35x10⁻⁶ ppm. The fluid saturated bulk modulus is estimated using Gassmann's equation (A5) while the fluid saturated shear modulus is same as the effective dry shear modulus.

The estimated and observed fluid saturated bulk and shear moduli are shown in Figure 2a and 2b, respectively. The corresponding P- and S-wave velocities are shown in Figure 2c and 2d, respectively. In general, the bulk modulus estimated from the EMM matches well with the observed bulk modulus. The bulk modulus is independent of friction as it depends only on normal force (F_n), and the friction between the grains affects only the tangential force (F_t). Interestingly, the shear modulus is accurately estimated for Walton's smooth model [$f(\mu)=0$], but it is overestimated by a factor of 2.5 for Hertz-Mindlin's no-slip model [$f(\mu)=1$]. The modeled P- and S-wave velocities show adequate match with the observed velocities for $f(\mu)=0$, but velocities are overestimated especially the S-wave velocity by a factor of 1.5 for $f(\mu)=1$ (Fig. 2d). Minor changes in P-wave velocity are observed for these end member frictional models as the estimated bulk modulus is significantly larger than the shear modulus. The present study shows that the Walton's smooth model (Walton, 1987) is more appropriate for estimating both the P- and S-wave velocities in a clay-dominated marine sediments. The comparison between the laboratory measured velocities on the synthetic granular samples and that estimated from EMM model also suggest that the Hertz-Mindlin's no-slip model vastly over predicts the shear modulus while the Walton's smooth model presents a better comparison (Zimmer et al., 2007). The analysis of log data from a shallow gas reservoir offshore Norway (Bachrach and Avseth, 2008) also shows the overestimate of shear modulus by a factor of 3 for $f_t=1$. They show that bulk and shear moduli are

accurately estimated for a lower friction value of $f_i = 0.07$. Thus, the classical Hertz–Mindlin (Mindlin, 1949) contact theory fails in predicting the shear modulus of shallow marine sediments when the friction between the grains is negligible.

4.2 Modified EMM for gas hydrate bearing sediments at Site NGHP–01–07

The presence gas hydrate in the marine sediments increases the P– and S–wave velocities. A rock physics model is required to estimate the variations of velocities with gas hydrate saturation. The EMM with smooth contact can reliably predict the velocities of background fluid saturated sediments at site NGHP–01–03. In this section, we extend the model to predict the velocities of gas hydrate bearing sediments at site NGHP–01–07 (Appendix B) following Helgerud et al. (1999) assuming that the hydrate can be modeled as load–bearing (hydrate as part of sediment matrix). We ignore the presence of hydrate within the pore space as it affects only the bulk modulus while the shear modulus remains unchanged and at this Site both P– and S–wave velocities increase with hydrate saturation. Several studies on gas hydrate formation worldwide also favors load–bearing hydrate (Lee and Waite, 2008; Lee and Collett, 2011; Wang et al., 2011). The interaction between the sediment grain and gas hydrate are studied by comparing the gas hydrate saturations estimated from sonic logs with that estimated from resistivity log and chloride anomaly.

The effective bulk and shear moduli of the solid frame are estimated assuming 80 % clay and 20 % quartz (Collett et al., 2008) using the elastic properties of individual mineral constituents as shown in Table–1. The P– and S–wave velocities estimated from EMM with Walton’s smooth model assuming load–bearing gas hydrate (Helgerud et al., 1999) are shown in Figure 3 for different hydrate saturations (10, 20 and 30 %) assuming two different friction parameters $f(\mu) = 0$ and $f(\mu) = 0.165$. Figure 3a shows the observed and modeled P–wave velocity for different gas hydrate saturations and the maximum gas hydrate saturation is 20 % just above the BSR; minor changes in gas hydrate saturation is observed for the two frictional models. Figure 3b shows the observed and modeled S–wave velocity for different gas hydrate saturations with the maximum gas hydrate saturation ~ 30 % for $f(\mu) = 0$ and ~ 20 % for $f(\mu) = 0.165$. The gas hydrate saturation as estimated by shear velocities is overestimated for zero-friction. Assuming a small friction between the grain contacts ($f(\mu) = 0.165$), the hydrate saturation estimated from shear velocities matches with that estimated from P– wave velocity at site

NGHP-01-07. The friction parameter is obtained by varying $f(\mu)$ from zero to unity and comparing the gas hydrate saturation estimated from both P- and S-wave velocities. The gas hydrate saturations are also estimated from resistivity data (Collett et al., 2008) and chloride anomaly using equation $S_h \approx \frac{\beta(C_{cb} - C_c)}{C_c + \beta(C_{cb} - C_c)}$ (Malinverno et al., 2008), where S_h is the amount of gas hydrate in pore space; C_{cb} is the in situ baseline pore water chlorinity; C_c represents the chlorinity measured in the core samples after gas hydrate dissociation; β is the dimensionless coefficient to account for the density change between gas hydrate to water and it is assumed to be equal to 1.257. The comparison of gas hydrate saturation from the sonic logs and resistivity log is shown within the gas hydrate stability zone (Figure 4). Ignoring the friction in EMM leads to under estimation of shear wave velocity for the gas hydrate bearing sediments; accounting for limited friction between the sediment grain and hydrate ($f(\mu) = 0.165$) predicts similar gas hydrate saturations from both P- and S-wave velocities and match well with those estimated from resistivity log and chloride anomalies. The difference in estimated and observed gas hydrate saturation from sonic and resistivity logs between 145 and 152 mbsf may be attributed to the high concentration of gas hydrate in fractures as observed in resistivity images (Collett et al., 2008).

The present study shows that the friction between the grain contacts cannot be ignored for gas hydrate bearing sediment. In general, formation of gas hydrate in sediments strengthens the host sediment and increases the cohesion which may lead to non-zero friction (Kleinberg and Dai, 2005). The cohesion of the sediment matrix with hydrate is strongly dependent on the type of gas hydrate morphology. For example, gas hydrate within the pore space may behave frictionless, and the contacts between the grains may be modeled with Walton's smooth model. The resultant S-wave velocity is almost constant and equals to that of the background fluid saturated sediments. However, load-bearing gas hydrate sediments may increase the cohesion between grain contacts, and therefore, cannot be modeled with Walton's smooth model. When the gas hydrate coats the sediment (cementation model), the cohesion increases rapidly even for low gas hydrate saturation leading to significantly high S-wave velocity (Kleinberg and Dai, 2005). The modified EMM model can reproduce this behavior by incorporating frictional forces between the sediment grain and gas hydrate. Guerin and Goldberg (2005) assumed that frictional force between sediment and gas hydrate are linear functions of the velocity differential between them, similar to viscous forces in fluid. Using these viscous frictional forces, they

accurately estimated the P- and S-wave velocities in the Mallik 5L-38 well. In the present study, we observe similar phenomena suggesting that the smooth models (with zero friction) leads to lower S-wave velocity and may have important consequences for AVO interpretation. However, the friction due to the presence of gas hydrate marginally affects the P-wave velocity, and therefore can be used effectively to calculate the gas hydrate saturations.

The EMM model was originally developed for the contact between the same grains. In the case of mixed mineralogy, homogeneous mineral moduli are usually derived using Hill's average (Hill, 1952) and these moduli are used for the calculation of effective dry bulk and shear moduli. However, if the elastic moduli of the mixed minerals are significantly different such an assumption breaks down (Avseth et al., 2005), and the contact model for the multiple type of grains needs to be developed. One such model is developed for a mixture of quartz and glauconite grains and is tested on laboratory as well as field data (Hossain et al., 2011). The detail of such a model is discussed in Appendix C. In the present study, we extended the EMM model for a mixture of three grains: quartz, clay and hydrate in the following section.

4.3 Modified EMM for the mixed grains: quartz, clay and gas hydrate

The two grain contact model for quartz and glauconite sediment grains has been developed in the North Sea in order to account for significantly different elastic moduli of the grains (Hossain et al., 2011). In such a model, the mineral's effective Young's modulus of quartz and glauconite contact is calculated from the elastic properties of the individual minerals following Johnson (1985) as,

$$E_{Eff(QG)} = \left(\frac{1-\nu_q}{2G_q} + \frac{1-\nu_g}{2G_g} \right)^{-1}, \quad (1)$$

where G_q and G_g are the shear modulus of quartz and glauconite, respectively; ν_q , ν_g are the Poisson's ratio of quartz and glauconite, respectively (Appendix C). For unequal mixture of quartz and glauconite, the effective modulus is estimated using weighted average for different grain contacts: quartz-quartz (QQ), quartz-glauconite (QG) and glauconite-glauconite (GG). The weights are assumed to be proportional to their volume fraction, and the sum of weights is assumed to be equal to unity. This effective Young's modulus is used for the calculation of effective dry bulk and shear moduli at critical

porosity assuming Hertz–Mindlin contact theory. The remaining procedure for calculating the P– and S–wave velocities remains similar to the classic effective medium model (Dvorkin et al., 1999).

We extend the grain contact method (Hossain et al., 2011) for gas hydrate bearing sediment because the significantly different elastic moduli of gas hydrate and clay/quartz may lead to the breakdown of Hill’s averaging equation (Hill, 1952). When gas hydrate acts as load–bearing (Helgerud et al., 1999), gas hydrate needs to be treated as a part of sediment matrix and the effective Young’s modulus needs to be estimated for three–grain contact (clay + quartz + gas hydrate). The possible contact combinations among the grains are quartz–quartz (QQ), clay–clay (CC), clay–quartz (QC), quartz–hydrate (QH), clay–hydrate (CH), and hydrate–hydrate (HH) assuming that the contacts are independent of each other. The effective Young’s modulus for different contact combinations can be estimated following Johnson (1985) as,

$$\begin{aligned}
 E_{Eff(QC)} &= \left(\frac{1-\nu_q}{2G_q} + \frac{1-\nu_c}{2G_c} \right)^{-1}, \\
 E_{Eff(QH)} &= \left(\frac{1-\nu_q}{2G_q} + \frac{1-\nu_h}{2G_h} \right)^{-1}, \\
 E_{Eff(CH)} &= \left(\frac{1-\nu_c}{2G_c} + \frac{1-\nu_h}{2G_h} \right)^{-1},
 \end{aligned} \tag{2}$$

where G_q , G_c and G_h are the shear modulus of quartz, clay and gas hydrate, respectively; ν_q , ν_c and ν_h are the Poisson’s ratio of quartz, clay and hydrate, respectively. If the grains are same, the effective Young’s modulus can be estimated using equation (3),

$$\begin{aligned}
 E_{Eff(QQ)} &= \frac{G_q}{1-\nu_q}, \\
 E_{Eff(CC)} &= \frac{G_c}{1-\nu_c}, \\
 E_{Eff(HH)} &= \frac{G_H}{1-\nu_H},
 \end{aligned} \tag{3}$$

where $E_{Eff(QQ)}$, $E_{Eff(CC)}$ and $E_{Eff(HH)}$ are the effective Young’s modulus of quartz–quartz, clay–clay and hydrate–hydrate contact, respectively. The effective Young’s modulus of the mixed grains can be

estimated by considering weighted average of all possible grain contacts assuming that the weights are proportional to the corresponding volume fractions (Hossain et al., 2011),

$$\begin{aligned}
E_{Eff(3)} = & \bar{f}_q (\bar{f}_q \cdot E_{Eff(QQ)} + \bar{f}_c \cdot E_{Eff(QC)} + \bar{f}_h \cdot E_{Eff(QH)}) \\
& + \bar{f}_c (\bar{f}_c \cdot E_{Eff(CC)} + \bar{f}_q \cdot E_{Eff(CQ)} + \bar{f}_h \cdot E_{Eff(CH)}) \\
& + \bar{f}_h (\bar{f}_h \cdot E_{Eff(HH)} + \bar{f}_q \cdot E_{Eff(QH)} + \bar{f}_c \cdot E_{Eff(CH)})
\end{aligned} \tag{5}$$

$$\begin{aligned}
E_{Eff(3)} = & \bar{f}_q^2 E_{Eff(QQ)} + \bar{f}_c^2 E_{Eff(CC)} + \bar{f}_h^2 E_{Eff(HH)} \\
& + 2\bar{f}_q \bar{f}_c E_{Eff(QC)} + 2\bar{f}_q \bar{f}_h E_{Eff(QH)} + 2\bar{f}_c \bar{f}_h E_{Eff(CH)},
\end{aligned}$$

where $E_{Eff(3)}$ is the effective Young's modulus of the quartz, clay and hydrate; \bar{f}_q , \bar{f}_c and \bar{f}_h are the effective volume fractions of quartz, clay, and hydrate due to the presence of load-bearing hydrate (Helgerud et al., 1999). The presence of hydrate reduces the original porosity ϕ to $\bar{\phi} = \phi - C_h$, where C_h is the volumetric concentration of gas hydrate in sediments. The effective volume fraction \bar{f}_q and \bar{f}_c are related to the original fraction (f_i) as,

$$\bar{f}_q = f_i (1 - \phi) / (1 - \bar{\phi}), \tag{6}$$

$$\bar{f}_c = f_i (1 - \phi) / (1 - \bar{\phi}),$$

and

$$\bar{f}_h = (C_h) / (1 - \bar{\phi}).$$

The effective dry bulk (K_{HM}) and shear (G_{HM}) moduli at critical porosity (ϕ_c) can be estimated from equation (B1) with arbitrary frictional parameter $f(\mu)$. The P- and S-wave velocities are then estimated following the classical EMM (Dvorkin et al., 1999; Appendix A).

The estimated baseline P- and S-wave velocities at Site NGHP-01-03 using modified EMM with mixed grain-contact is similar to that estimated from EMM (Fig. 3a) suggesting that the difference between the elastic moduli of mineral components (quartz and clay) is not great enough to produce

noticeable change in the velocities. The modeled P- and S-wave velocities at site NGHP-01-07 for different gas hydrate saturations (10, 20 and 30 %) after accounting for the same friction parameter ($f(\mu)=0.165$) and the mixed grain contact (Hossain et al., 2011) are shown in Figure 5a and 5b, respectively. Accounting for mixed grain contact in EMM does not lead to significant changes in the P-wave velocity. However, shear velocities seem to be overestimated and the differences seem to be increasing with hydrate saturations. The maximum gas hydrate saturation is estimated to be around 10 % assuming the same friction parameter but with mixed grain contact. Thus, the gas hydrate saturations estimated from S-wave velocities are underestimated by 50 % as compared to those estimated from P-wave velocity as well as from the resistivity and chloride data. Further, we attempt to model the P- and S-wave velocities for different gas hydrate saturations (10, 20 and 30%) assuming zero friction in the modified EMM and the results are shown in Figure 6. The hydrate saturations estimated from P- and S-wave velocities along with those estimated from the resistivity and chloride data are shown in Figure 7. Interestingly, the gas hydrate saturations estimated from both the P-wave and S-wave velocities are comparable with the maximum gas hydrate saturation of ~20 % just above the BSR. The estimated saturations are in good agreement with those estimated from the resistivity log and chloride anomaly (Fig. 7). Therefore, the modified grain-contact EMM does not require any arbitrary friction parameter to match the gas hydrate saturations estimated from shear wave velocity. In other words, if the mixed grain contact is not accounted in the EMM it leads to non-zero friction parameter for gas hydrate bearing sediments.

5. Conclusion

Log data acquired during NGHP Expedition-01 are used to study the first principle rock physics model including the effective medium model for clay-dominated, unconsolidated marine sediments as well as gas hydrate bearing sediments in KG basin. The background fluid-saturated P- and S-wave velocities are studied at Site NGHP-01-03, where negligible gas hydrate amount is observed. The modeled P- and S-wave velocities match the observed velocities for $f(\mu)=0$ (Walton's smooth model); however, the S-wave velocity is overestimated by factor of 1.5 for $f(\mu)=1$ (Hertz-Mindlin contact model) due to inaccuracy in estimating the effective tangential stiffness. Using Walton's smooth model in EMM, the gas hydrate saturations are estimated from P- and S-wave velocities at Site NGHP-01-07, which represents load-bearing gas hydrate deposits. The gas hydrate saturations estimated from P-wave

velocity match well with those estimated from resistivity and chloride anomaly; however, the gas hydrate saturations estimated from S-wave velocity are overestimated indicating underestimation of shear modulus. This mismatch is corrected by incorporating arbitrary friction parameter in the EMM which largely affect the saturations estimated only from S-wave velocity. The EMM is again modified to account for mixed grain contact as the elastic moduli of gas hydrate are significantly different from that of the background clay/quartz minerals. The model is tested at Site NGHP-01-07 assuming the same friction parameter. The gas hydrate saturations estimated from P-wave do not vary significantly; however, the saturations estimated from shear velocity are underestimated by ~50% as compared to other estimates. Interestingly, the hydrate saturations estimated assuming zero friction (Walton's smooth contact) are comparable to those estimated from resistivity and chloride data. Thus the modified EMM with zero friction and mixed grain contact is able to predict the velocities of fluid-saturated sediments at site NGHP-01-03 as well as gas hydrate bearing sediments at Site NGHP-01-07.

Acknowledgements

The authors wish to thank those that contributed to the success of the National Gas Hydrate Program Expedition 01 (NGHP-01). NGHP-01 was planned and managed through collaboration between the Directorate General of Hydrocarbons (DGH) under the Ministry of Petroleum and Natural Gas (India), the U.S. Geological Survey (USGS), and the Consortium for Scientific Methane Hydrate Investigations (CSMHI) led by Overseas Drilling Limited (ODL) and FUGRO McClelland Marine Geosciences (FUGRO). The platform for the drilling operation was the research drill ship *JOIDES Resolution*, operated by ODL. Much of the drilling/coring equipment used was provided by the Integrated Ocean Drilling Program (IODP) through a loan agreement with the US National Science Foundation. Wireline pressure coring systems and supporting laboratories were provided by IODP/Texas A&M University (TAMU), FUGRO, USGS, U.S. Department of Energy (USDOE) and HYACINTH/GeoTek. Downhole logging operational and technical support was provided by Lamont-Doherty Earth Observatory (LDEO) of Columbia University. The financial support for the NGHP-01, from the Oil Industry Development Board, Oil and Natural Gas Corporation Ltd., GAIL (India) Ltd. and Oil India Ltd. is gratefully acknowledged. We also acknowledge the support extended by all the participating organizations of the NGHP: MoP&NG, DGH, ONGC, GAIL, OIL, NIO, NIOT, and RIL. The Director of National Institute of Oceanography (NIO) is thanked for encouragement, support and the permission to publish. We would like to thank the reviewers for providing useful comments/suggestions which has improved the quality of the manuscript. This is NIO contribution no. xxx.

Appendix A: Effective medium model (Dvorkin et al., 1999; Helgerud et al., 1999)

The effective bulk (K) and shear (G) modulus of the solid phase at zero porosity is estimated from individual mineral constituents using the Hill's average (Hill, 1952).

$$\begin{aligned} K &= \frac{1}{2} \left[\sum_{i=1}^m f_i K_i + \left(\sum_{i=1}^m f_i / K_i \right)^{-1} \right], \\ G &= \frac{1}{2} \left[\sum_{i=1}^m f_i G_i + \left(\sum_{i=1}^m f_i / G_i \right)^{-1} \right], \end{aligned} \quad (\text{A1})$$

where K_i and G_i are the bulk and shear modulus of individual mineral constituent; f_i is the volume fraction of individual mineral constituents. The effective dry bulk (K_{HM}) and shear (G_{HM}) moduli at

critical porosity (ϕ_c) can be estimated as,

$$\begin{aligned} K_{HM} &= \left[\frac{n^2 (1 - \phi_c)^2 G^2}{18\pi^2 (1 - \nu^2)} P \right]^{\frac{1}{3}}, \\ G_{HM} &= \frac{5 - 4\nu}{5(2 - \nu)} \left[\frac{3n^2 (1 - \phi_c)^2 G^2}{2\pi^2 (1 - \nu)^2} P \right]^{\frac{1}{3}}, \end{aligned} \quad (\text{A2})$$

where P is the effective pressure defined as the difference between the lithostatic and hydrostatic pressure, and can be represented as $P = (\rho_b - \rho_w)gD$; ρ_b and ρ_w are sediment and water density, respectively; g is the acceleration due to gravity; D is the depth below seafloor; K , G are the effective bulk and shear modulus of the solid phase, respectively; ν_{dry} is the effective Poisson's ratio of the dry medium; n is the coordination number (average number of grain contacts per grain) which can be represented as a function of porosity (ϕ) (Zimmer, 2003),

$$n = 24e^{(-2.547\phi)} - 0.373. \quad (\text{A3})$$

The effective dry bulk and shear modulus at other porosity is estimated based on the Hashin–Shtrikman (1963) bounds,

$$\begin{aligned}
K_{Dry} &= \left[\frac{\phi/\phi_c}{K_{HM} + \frac{4}{3}G_{HM}} + \frac{1-\phi/\phi_c}{K + \frac{4}{3}G_{HM}} \right]^{-1} - \frac{4}{3}G_{HM}, \\
G_{Dry} &= \left[\frac{\phi/\phi_c}{G_{HM} + Z} + \frac{1-\phi/\phi_c}{G + Z} \right]^{-1} - Z, \quad \phi < \phi_c \\
Z &= \frac{G_{HM}}{6} \left(\frac{9K_{HM} + 8G_{HM}}{K_{HM} + 2G_{HM}} \right), \tag{A4}
\end{aligned}$$

$$\begin{aligned}
K_{Dry} &= \left[\frac{(1-\phi)/(1-\phi_c)}{K_{HM} + \frac{4}{3}G_{HM}} + \frac{(\phi-\phi_c)/(1-\phi_c)}{\frac{4}{3}G_{HM}} \right]^{-1} - \frac{4}{3}G_{HM}, \quad \phi \geq \phi_c \\
G_{Dry} &= \left[\frac{(1-\phi)/(1-\phi_c)}{G_{HM} + Z} + \frac{(\phi-\phi_c)/(1-\phi_c)}{Z} \right]^{-1} - Z.
\end{aligned}$$

The bulk modulus (K_{sat}) of fluid saturated sediment is estimated using the Gassmann's equation (Gassmann, 1951),

$$\begin{aligned}
K_{Sat} &= K \frac{\phi K_{Dry} - (1-\phi)K_f K_{Dry} / K + K_f}{(1-\phi)K_f + \phi K - K_f K_{Dry} / K} \\
G_{Sat} &= G_{Dry} \tag{A5}
\end{aligned}$$

The P- and S-wave velocities are calculated as,

$$\begin{aligned}
V_P &= \sqrt{\frac{K_{sat} + \frac{4}{3}G_{sat}}{\rho}}, \\
V_S &= \sqrt{\frac{G_{sat}}{\rho}}. \tag{A6}
\end{aligned}$$

The presence of gas hydrate in the pore space affects only bulk modulus; the shear modulus remains unchanged. If hydrate acts as load-bearing, it acts as a part of sediment matrix and alters both

bulk and shear moduli (Helgerud et al., 1999). The effective bulk and shear modulus is obtained using Hill's average,

$$K = \frac{1}{2} \left[\sum_{i=1}^m \bar{f}_i K_i + \left(\sum_{i=1}^m \bar{f}_i / K_i \right)^{-1} \right]$$

$$G = \frac{1}{2} \left[\sum_{i=1}^m \bar{f}_i G_i + \left(\sum_{i=1}^m \bar{f}_i / G_i \right)^{-1} \right]$$
(A7)

where \bar{f}_i is the new volume fraction of the sediment matrix due to the presence of gas hydrate and is given by $\bar{f}_i = f_i (1 - \phi) / (1 - \bar{\phi})$; $\bar{\phi}$ is the reduced porosity defined as $\bar{\phi} = \phi - C_h$, where C_h is the volumetric concentration of gas hydrate. The volume fraction of gas hydrate is defined by $\bar{f}_h = C_h / (1 - \bar{\phi})$. The effective dry bulk and shear moduli at critical porosity is given by equation (A2), and the effective dry bulk and shear modulus at any other porosity is given by equation (A4). The fluid saturated bulk and shear moduli are given by equation (A5) and the velocities by equation (A6).

Appendix B: Friction dependent EMM (Duffaut et al., 2010)

In classic EMM model (Dvorkin et al., 1999), the effective dry bulk and shear moduli at critical porosity are estimated using Hertz–Mindlin contact theory (Mindlin, 1949). Such contact theory assumes no–slip across the grain contact. Duffaut et al. (2010) extended the EMM by introducing partial slip with non–zero contact friction given by a free parameter Mindlin friction term $f(\mu)$ which represents the ratio between the radius of no–slip grain contact and the grain. In the frictional dependent model, the effective dry shear modulus of the identical sphere pack is derived by combining the tangential contact stiffness estimated from extended Mindlin’s theory (Mindlin, 1949) with the effective modulus derived by Digby (1981) and can be represented as,

$$\begin{aligned}
 K_{dry} &= \left[\frac{(1-\phi_c^2)G^2}{18\pi^2(1-\nu^2)} \left(n^2 \frac{\bar{R}}{R} \right) P \right]^{\frac{1}{3}} \\
 G_{dry} &= \frac{3}{5} \left[1 + \frac{3(1-\nu)}{2-\nu} f(\mu) \right] K_{dry} \\
 f(\mu) &= \frac{1}{3} \left(\frac{2-\nu_{dry}}{1-\nu_{dry}} \right) \left(\frac{5}{3} \frac{G}{K} - 1 \right)
 \end{aligned} \tag{B1}$$

Appendix C: Mixed grain–contact EMM (Hossain et al., 2011)

In classical EMM (Dvorkin et al., 1999), the effective moduli of mixed grains are calculated from the homogeneous mineral moduli derived from Hill’s average (Hill, 1952) and these moduli are used for the calculation of effective dry bulk and shear moduli. In order to account for mixed grains, Hossain et al. (2011) developed a modified EMM and tested it for a mixture of quartz and glauconite grains on laboratory as well as field data. In this model, the mineral’s effective Young’s modulus of quartz and glauconite contact is calculated from the elastic properties of the individual minerals following Johnson (1985) as,

$$E_{Eff(QG)} = \left(\frac{1-\nu_q}{2G_q} + \frac{1-\nu_g}{2G_g} \right)^{-1}, \tag{C1}$$

where G_q and G_g are the shear modulus of quartz and glauconite, respectively; ν_q , ν_g are the Poisson's ratio of quartz and glauconite, respectively. If the material of the two grain are similar, equation (C1) reduces to,

$$E_{Eff(QQ)} = \frac{G_q}{1-\nu_q} \tag{C2}$$

$$E_{Eff(GG)} = \frac{G_g}{1-\nu_g}$$

where $E_{Eff(QQ)}$ and $E_{Eff(CC)}$ are the effective Young's modulus of quartz–quartz contact and glauconite–glauconite contact, respectively. For unequal mixture of quartz and glauconite, the effective modulus is estimated using weighted average for different grain contacts: quartz–quartz (QQ), quartz–glauconite (QG) and glauconite–glauconite (GG). The weights are assumed to be proportional to their volume fraction, and the sum of weights is assumed to be equal to unity,

$$E_{Eff(2)} = f_q(f_q \cdot E_{Eff(QQ)} + f_g \cdot E_{Eff(QG)}) + f_g(f_g \cdot E_{Eff(GG)} + f_q \cdot E_{Eff(GQ)}) \tag{C3}$$

$$E_{Eff(2)} = f_q^2 E_{Eff(QQ)} + f_g^2 E_{Eff(GG)} + 2f_q f_g E_{Eff(QG)}$$

The effective dry bulk and shear moduli for two–grain contact is given by Hertz–Mindlin contact theory (Mindlin, 1949);

$$K_{dry} = \left[\frac{n^2 (1-\phi)^2 E_{Eff(2)}^2 P}{18\pi^2} \right]^{\frac{1}{3}},$$

$$G_{dry} = \frac{3(5-4\nu_{eff})K_{dry}}{5(2-\nu_{eff})}, \tag{C4}$$

where ν_{eff} is the effective Poisson's ratio of the grain mixture.

Table Caption

Table 1. Physical properties of clay, quartz, gas hydrate and water used for modeling the P- and S-wave velocities of gas hydrate bearing sediments (Helgerud et al., 1999).

Figures Caption

Figure.1. Location map of the study area in the Krishna—Godavari (KG) offshore basin. The zoom out of the study area with bathymetry data (Source: <http://www.ngdc.noaa.gov/>). The Sites NGHP-01-03 and NGHP-01-07, drilled by the JOIDES Resolution, are highlighted on the map.

Figure.2. Modeled versus well-log observations from Site NGHP-01-03: (a) bulk modulus from log data (black), modeled fluid saturated bulk modulus (GPa) for $f(\mu)=0$ and $f(\mu)=1$, (b) shear modulus from log data (black), modeled fluid saturated shear modulus (GPa) for $f(\mu)=0$ and $f(\mu)=1$, (c) P-wave velocity from log data (black), modeled P-wave velocity for $f(\mu)=0$ and $f(\mu)=1$, (d) S-wave velocity from log data (black), modeled S-wave velocity for $f(\mu)=0$ and $f(\mu)=1$.

Figure.3. Modeled versus well-log observations from Site NGHP-01-07: (a) observed and modeled P-wave velocity for varying gas hydrate saturations (0, 10, 20 and 30%) for $f(\mu)=0$ and $f(\mu)=0.165$, (b) observed and modeled S-wave velocity for varying gas hydrate saturations (0, 10, 20 and 30%) for $f(\mu)=0$ and $f(\mu)=0.165$. The gray box represents the region from 188 to 260 mbsf which is below the BSR and possibly has the presence of free gas.

Figure.4. Comparison among the gas hydrate saturations estimated from P- and S-wave velocities from EMM with friction parameter, resistivity and chloride anomaly: (a) gas hydrate saturation estimated from P-wave velocity for $f(\mu)=0.165$ and from resistivity and chloride anomaly, (b) gas hydrate saturation estimated from S-wave velocity for $f(\mu)=0.165$ and from resistivity and chloride anomaly.

Figure.5. Modeled versus observed P- and S-wave velocities at Site NGHP-01-07: (a) observed and modeled P-wave velocity for varying gas hydrate saturations (0, 10, 20 and 30%) using three grain contact EMM model with friction ($f(\mu)=0.165$), (b) observed and modeled S-wave velocity for varying gas hydrate saturations (0, 10, 20 and 30%) using three grain contact EMM model with friction ($f(\mu)=0.165$).

Figure.6. Modeled versus observed P- and S-wave velocities at Site NGHP-01-07: (a) observed and modeled P-wave velocity for varying gas hydrate saturations (0, 10, 20 and 30%) using three grain contact EMM model without friction, (b) observed and modeled P-wave velocity for varying gas hydrate saturations (0, 10, 20 and 30%) using three grain contact EMM model without friction.

Figure.7. Comparison among the gas hydrate saturations estimated from P- and S-wave velocities from EMM assuming zero friction and mixed grain contact, resistivity and chloride anomaly.

References

- Archie, G.E., 1942. The electrical resistivity log as an aid in determining some reservoir characteristics. *Trans. AIME* 146, 54–67.
- Avseth, P., Mukerji, T., Mavko, G., 2005. *Quantitative seismic interpretation: Applying rock physics tools to reduce interpretation risk*. Cambridge University Press.
- Bachrach, R., Avseth, P., 2008. Rock physics modeling of unconsolidated sands: Accounting for nonuniform contacts and heterogeneous stress fields in the effective media approximation with applications to hydrocarbon exploration. *Geophysics* 73, E197–E209.
- Backus, G.E., 1962. Long-wave elastic anisotropy produced by horizontal layering 67, 4427–4440.
- Batzle, M., Wang, Z., 1992. Seismic properties of pore fluids. *Geophysics* 57, 1396–1408.
- Carcione, J.M., Tinivella, U., 2000. Bottom-simulating reflectors: Seismic velocities and AVO effects. *Geophysics* 65, 54–67.
- Chand, S., Minshull, T. a., Gei, D., Carcione, J.M., 2004. Elastic velocity models for gas-hydrate-bearing sediments-a comparison. *Geophys. J. Int.* 159, 573–590.
- Collett, T.S., et al, 2008. Results of the Indian National Gas Hydrate Program Expedition-01 Initial Reports. Report, Director General of Hydrocarbons, Ministry of Petroleum and Natural Gas, New Delhi.
- Collett, T.S., et al., (this volume), Scientific Results of the National Gas Hydrate Program Expedition.
- Digby, P.J., 1981. The Effective Elastic Moduli of Porous Granular Rocks. *J. Appl. Mech.* 48, 803–808.
- Duffaut, K., Landrø, M., Sollie, R., 2010. Using Mindlin theory to model friction-dependent shear modulus in granular media. *Geophysics* 75, E143–E152.
- Dvorkin, J., Prasad, M., Sakai, A., Lavoie, D., 1999. Elasticity of marine sediments: Rock physics modeling. *Geophys. Res. Lett.* 26, 1781–1784.
- Ecker, C., Dvorkin, J., Nur, A., 1998. Sediments with gas hydrates: Internal structure from seismic AVO. *Geophysics* 63, 1659–1669.
- Goddard, J.D., 1990. Nonlinear elasticity and pressure-dependent wave speeds in granular media. *Proc. R. Soc. London. Ser. A Math. Phys. Sci.* 430, 105–131.
- Guerin, G., Goldberg, D., 2005. Modeling of acoustic wave dissipation in gas hydrate-bearing sediments. *Geochemistry, Geophys. Geosystems* 6, Q07010.

- Hashin, Z., Shtrikman, S., 1963. A variational approach to the theory of the elastic behaviour of multiphase materials. *J. Mech. Phys. Solids* 11, 127–140.
- Helgerud, M.B., Dvorkin, J., Nur, A., Sakai, A., Collett, T., 1999. Elastic-wave velocity in marine sediments with gas hydrates: Effective medium modeling. *Geophys. Res. Lett.* 26, 2021–2024.
- Hill, R., 1952. The elastic behaviour of a crystalline aggregate. *Proc. Phys. Soc. Sect. A* 65, 349.
- Hossain, Z., Mukerji, T., Dvorkin, J., Fabricius, I.L., 2011. Rock physics model of glauconitic greensand from the North Sea. *Geophysics* 76, E199–E209.
- Hyndman, R.D., Spence, G.D., 1992. A seismic study of methane hydrate marine bottom simulating reflectors. *J. Geophys. Res.* 97, 6683–6698.
- Inks, T., Lee, M., Agena, W., Taylor, D., Collett, T., Hunter, R., Zyrianova, M., 2009. Prospecting for gas hydrate accumulations using 2-D and 3-D seismic data, Milne Point, North Slope, Alaska. *Nat. Gas Hydrates---Energy Resour. Potential Assoc. Geol. Hazards AAPG Mem.* 89, 1–29.
- Jakobsen, M., Hudson, J.A., Minshull, T.A., Singh, S.C., 2000. Elastic properties of hydrate-bearing sediments using effective medium theory. *J. Geophys. Res.* 105, 561–577.
- Johnson, K.L., 1985. *Contact mechanics*. Cambridge University Press.
- Kleinberg, R., Dai, J., 2005. Estimation of the mechanical properties of natural gas hydrate deposits from petrophysical measurements, in: *Offshore Technology Conference, OTC 17205*.
- Kumar, D., Dash, R., Dewangan, P., 2009. Methods of gas hydrate concentration estimation with field examples. *Geo-Horizons* 76–86.
- Kumar, P., et al., (this volume), *National Gas Hydrate Program Expedition 01: Krishna-Godavari Operational and Technical Summary*.
- Lee, M.W., 2002. Biot–Gassmann theory for velocities of gas hydrate-bearing sediments. *Geophysics* 67, 1711–1719.
- Lee, M.W., Collett, T.S., 2011. In-situ gas hydrate saturation estimated from various well logs at the Mount Elbert Gas Hydrate Stratigraphic Test Well, Alaska North Slope. *Mar. Pet. Geol.* 28, 439–449.
- Lee, M.W., Waite, W.F., 2008. Estimating pore-space gas hydrate saturations from well log acoustic data. *Geochemistry, Geophys. Geosystems* 9, 1–8.
- Makse, H.A., Gland, N., Johnson, D.L., Schwartz, L.M., 1999. Why effective medium theory fails in granular materials. *Phys. Rev. Lett.* 83, 5070–5073.

- Malinverno, A., Kastner, M., Torres, M.E., Wortmann, U.G., 2008. Gas hydrate occurrence from pore water chlorinity and downhole logs in a transect across the northern Cascadia margin (Integrated Ocean Drilling Program Expedition 311). *J. Geophys. Res.* 113, B08103.
- Mindlin, R.D., 1949. Compliance of bodies in contact. *J. Appl. Mech.* 16, 259–268.
- Pride, S.R., Berryman, J.G., Harris, J.M., 2003. Seismic attenuation due to wave-induced flow 1–18.
- Pride, S.R., Berryman, J.G., Harris, J.M., 2004. Seismic attenuation due to wave-induced flow. *J. Geophys. Res. Solid Earth* 109.
- Singh, S.C., Minshull, T.A., Spence, G.D., 1993. Velocity structure of a gas hydrate reflector. *Science* (80-.). 260, 204–207.
- Sloan, E.D., 1998. *Clathrate Hydrates of Natural Gases* (second ed.), MarcelDekker, New York. Marcel Dekker, New York.
- Sriram, G., Dewangan, P., Ramprasad, T., Rama Rao, P., 2013. Anisotropic amplitude variation of the bottom-simulating reflector beneath fracture-filled gas hydrate deposit. *J. Geophys. Res. Solid Earth* 118, 2258–2274.
- Walton, K., 1987. The effective elastic moduli of a random packing of spheres. *J. Mech. Phys. Solids* 35, 213–226.
- Wang, X., Hutchinson, D.R., Wu, S., Yang, S., Guo, Y., 2011. Elevated gas hydrate saturation within silt and silty clay sediments in the Shenhu area, South China Sea. *J. Geophys. Res.* 116, B05102.
- Winkler, K.W., 1983. Contact stiffness in granular porous materials: comparison between theory and experiment. *Geophys. Res. Lett.* 10, 1073–1076.
- Zimmer, M., 2003. *Seismic velocities in unconsolidated sands: Measurements of pressure, sorting, and compaction effects.* PhD Thesis, Stanford University.
- Zimmer, M.A., Prasad, M., Mavko, G., Nur, A., 2007. Seismic velocities of unconsolidated sands: Part 1- Pressure trends from 0.1 to 20 MPa. *Geophysics* 72, E1–E13.

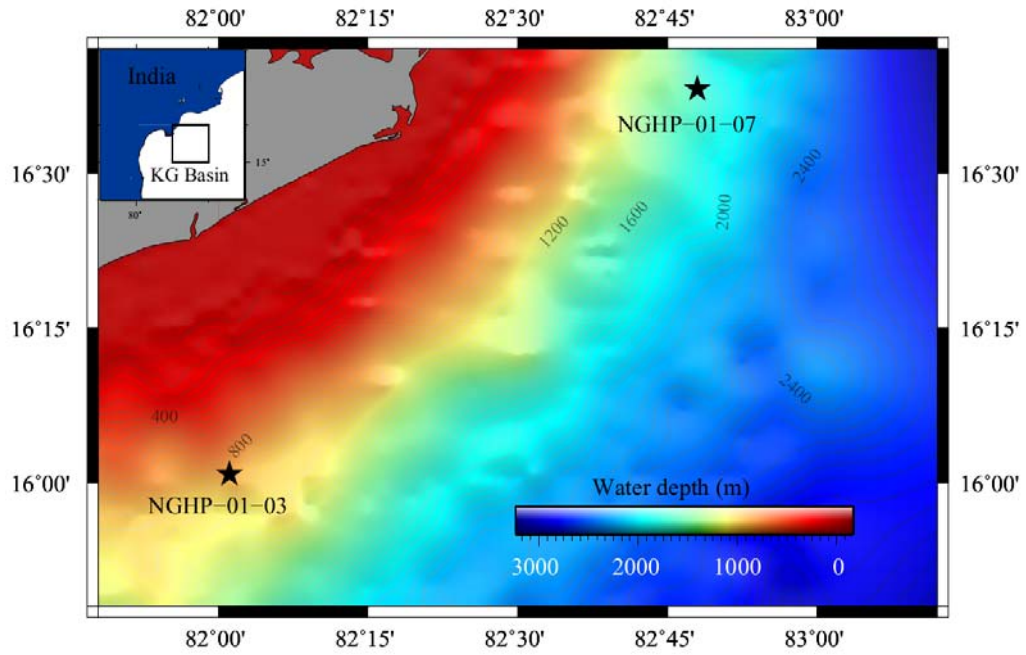


Figure 1

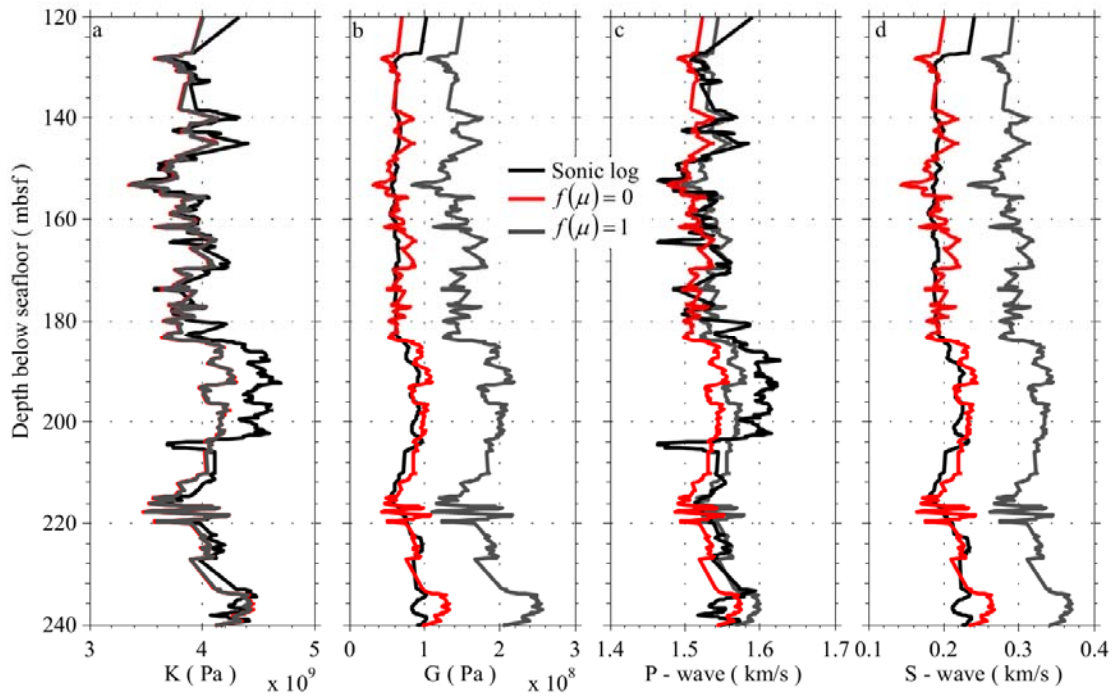


Figure 2

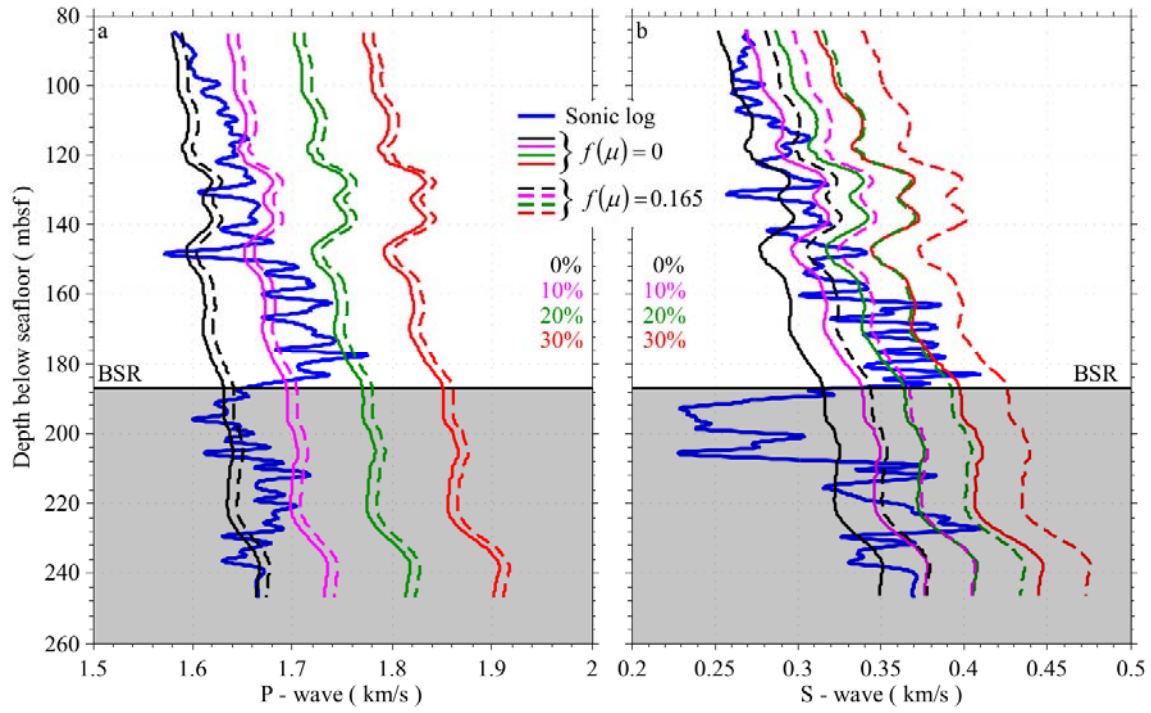


Figure 3

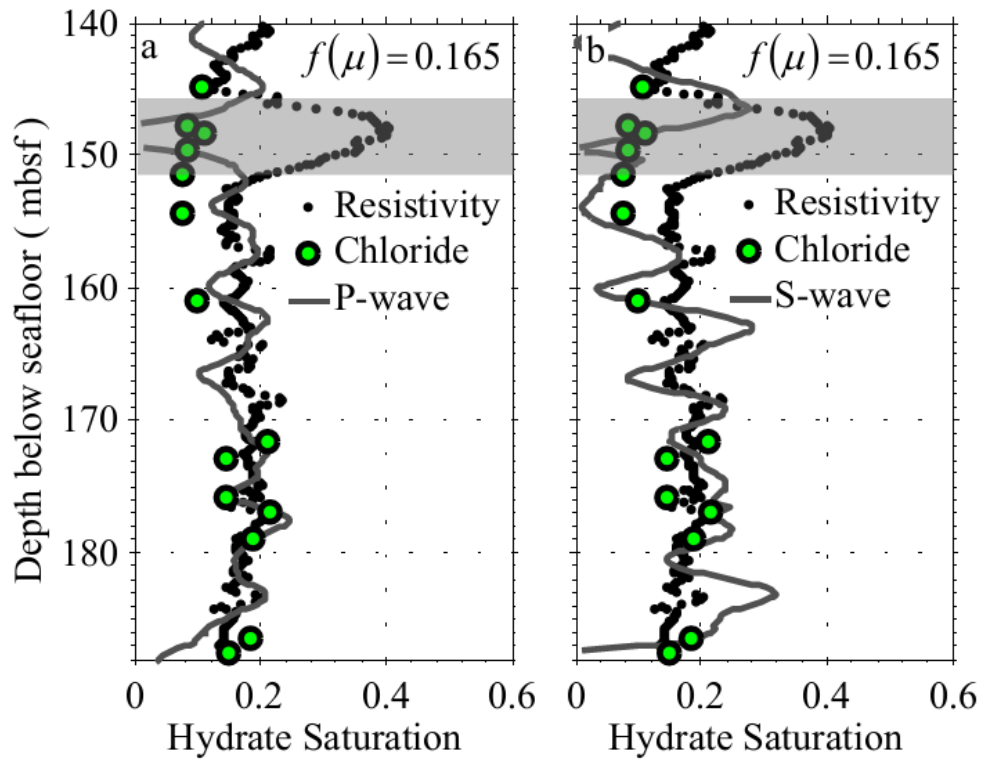


Figure 4

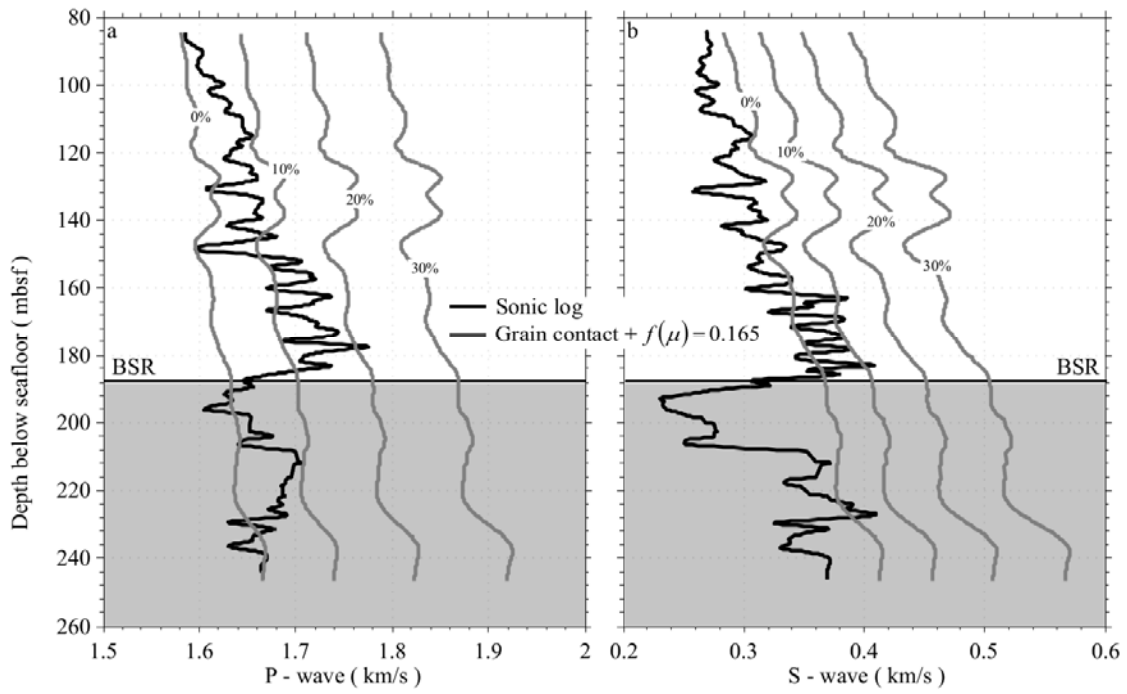


Figure 5

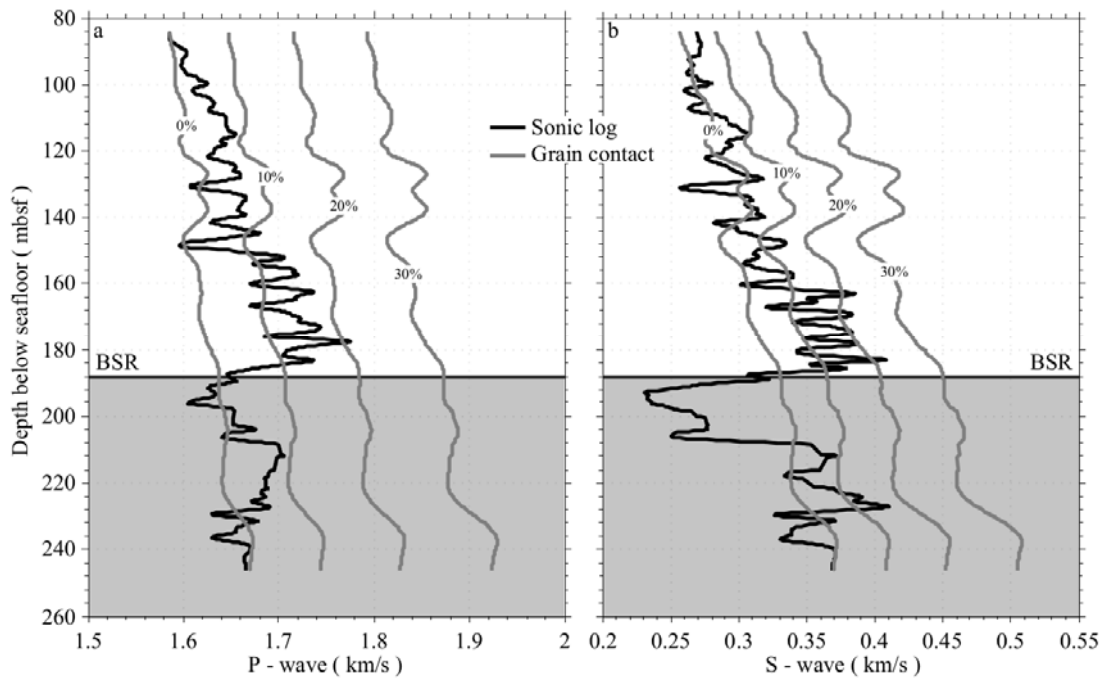


Figure 6

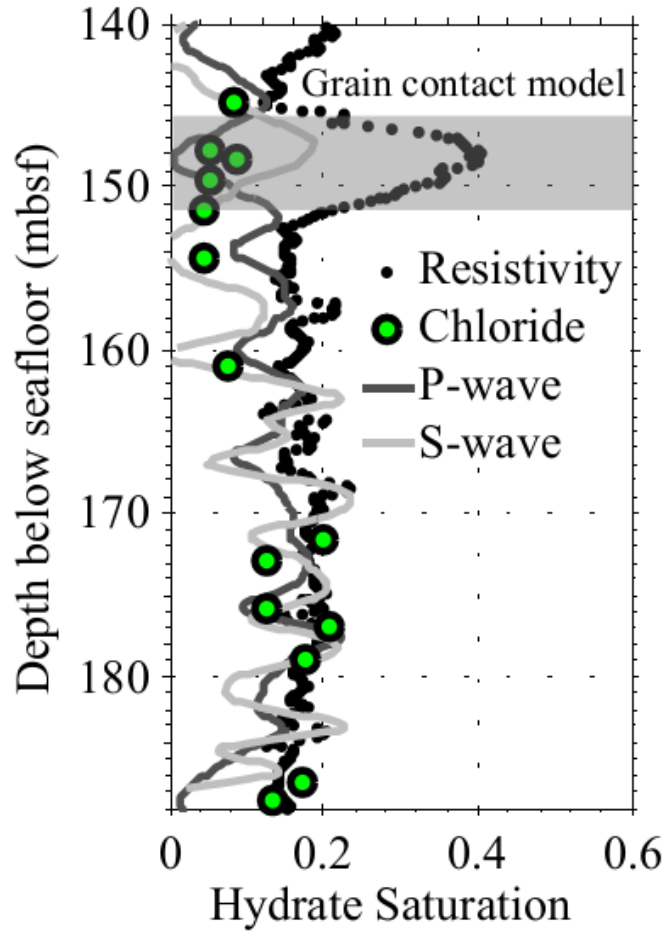


Figure 7

Mineral Constituent	Bulk Modulus 'K' (GPa)	Shear Modulus 'G' (GPa)	Density ' ρ' ' (g/cm ³)
Clay	20.9	6.85	2.58
Quartz	36.6	45	2.65
Gas Hydrate	7.9	3.3	0.90
Water	2.4.-2.6	0	1.032

Table 1